Fast and Slow Gating Relaxations in the Muscle Chloride Channel CLC-1

Alessio Accardi and Michael Pusch

From the Istituto di Cibernetica e Biofisica, Consiglio Nazionale delle Ricerche, Via de Marini 6, I-16149 Genova, Italy

abstract Gating of the muscle chloride channel CLC-1 involves at least two processes evidenced by double-exponential current relaxations when stepping the voltage to negative values. However, there is little information about the gating of CLC-1 at positive voltages. Here, we analyzed macroscopic gating of CLC-1 over a large voltage range (from −160 to +200 mV). Activation was fast at positive voltages but could be easily followed using envelope protocols that employed a tail pulse to −140 mV after stepping the voltage to a certain test potential for increasing durations. Activation was biexponential, demonstrating the presence of two gating processes. Both time constants became exponentially faster at positive voltages. A similar voltage dependence was also seen for the fast gate time constant of CLC-0. The voltage dependence of the time constant of the fast process of CLC-1, τ_f, was steeper than that of the slow one, τ_s (apparent activation valences were $z_f \sim -0.79$ and $z_s \sim -0.42$) such that at +200 mV the two processes became kinetically distinct by almost two orders of magnitude ($\tau_f \sim 16$ μs, $\tau_s \sim 1$ ms). This voltage dependence is inconsistent with a previously published gating model for CLC-1 (Fahlke, C., A. Rosenbohm, N. Mitrovic, A.L. George, and R. Rüdel. 1996. *Biophys. J.* 71:695–706). The kinetic difference at 200 mV allowed us to separate the steady state open probabilities of the two processes assuming that they reflect two parallel (not necessarily independent) gates that have to be open simultaneously to allow ion conduction. Both open probabilities could be described by Boltzmann functions with gating valences around one and with nonzero "offsets" at negative voltages, indicating that the two "gates" never close completely. For comparison with single channel data and to correlate the two gating processes with the two gates of CLC-0, we characterized their voltage, pH_{int}, and $[Cl]_{ext}$ dependence, and the dominant myotonia inducing mutation, I290M. Assuming a double-barreled structure of CLC-1, our results are consistent with the identification of the fast and slow gating processes with the single-pore and the common-pore gate, respectively.

key words: CLC-0 • fast gate • slow gate • double barreled • anion channel

INTRODUCTION

ClC proteins form a class of voltage-dependent Cl^- channels with several members involved in various hereditary human diseases. The chloride channel from the electric organ of the *Torpedo* ray, CLC-0 (Jentsch et al., 1990), was the first protein of this family to be cloned. The muscle channel, CLC-1, was soon thereafter identified (Steinmeyer et al., 1991). CLC-0 has a very peculiar appearance, it has three equidistant conductance levels of ~0, 8, and 16 pS. This behavior has been proposed to be due to a double-barreled structure: the channel is a dimer with two distinct, independently gating protopores and a common gate that modulates both protopores simultaneously (Miller, 1982; Ludewig et al., 1996; Middleton et al., 1996). Another peculiarity of CLC-0 is the fact that it has no evident voltage-sensing region similar to the S4 region in K^+ or Na^+ channels, but, on the contrary, it has been proposed (Pusch et al., 1995a; Chen and Miller, 1996) that the permeating ion itself acts as the gating particle. While other ClC channels also have a dimeric structure (Fahlke et al., 1997; Maduke et al., 1999), a demonstration of their double-barreled structure has been more difficult. CLC-0 and CLC-1 have ~50% sequence identity and on the macroscopic level CLC-0 and CLC-1 have many common properties, such as similar ion selectivity and similar fast deactivation kinetics. At the single-channel level, however, CLC-1 is much more difficult to study due to its small single-channel conductance.

Recently, Saviane et al. (1999) have advanced the proposal that the muscle chloride channel, CLC-1, also has a double-barreled structure based on single-channel measurements showing three equidistant conductance levels. Fluctuations between these states, at negative voltages, could be well described by a double-barreled structure with two independent single protopore fast gates and a single common pore slow gate. Based on macroscopic measurements, by contrast, Fahlke et al. (1996, 1998) have proposed for CLC-1 a completely different architecture with a single permeation pore and a different gating mechanism with two "classical" voltage-sensing regions that can move between two possible states and reach equilibrium on a very fast time scale ("ultrafast gate").

To test these various hypothesis and to possibly correlate the gating of CLC-1 to its putative double-barreled structure, we studied it in more detail in an extended voltage range. Using envelope protocols, we show here

Address correspondence to Michael Pusch, Istituto di Cibernetica e Biofisica, CNR, Via de Marini 6, I-16149 Genova, Italy. Fax: 39 0106475 500; E-mail pusch@barolo.icb.ge.cnr.it

that CLC-1 has two gating processes with voltage-dependent time constants. At negative voltages, both processes are slow, show little voltage dependence and have similar kinetics. Rising the applied voltage quickens both processes, although to a different extent, such that at V = +200 mV the time constants become almost two orders of magnitude different. The time constants do not show any appreciable saturation even at very high voltages.

It is known that, for CLC-0, lowering the internal pH rises the open probability of the fast gate (Hanke and Miller, 1983), while lowering the external chloride concentration induces a shift towards positive potentials of the open probability of the fast gate (Pusch et al., 1995a). Rychkov et al. (1996) have shown that the apparent open probability of CLC-1 is similarly affected by lowering internal pH and external chloride concentration. The dominant myotonia-inducing mutation, I290M, causes a positive shift of the open probability of the voltage dependence of the channel (Pusch et al., 1995b; Saviane et al., 1999). In the present work, we exploit the pronounced kinetic difference of the two gating processes at high voltages to separate them and investigate how they are individually affected by such variations of the experimental conditions.

MATERIALS AND METHODS

Current Recording

CLC-0 (Jentsch et al., 1990) and human CLC-1 (Koch et al., 1992) were expressed in *Xenopus* oocytes and currents were measured at 18°C 2–5 d after injection using the inside-out configuration of the patch-clamp technique (Hamill et al., 1981) with an EPC-7 amplifier (List) and the acquisition program Pulse (HEKA). Pipettes were pulled from aluminosilicate glass capillaries and had resistances of 1–4 MΩ. Pipettes were coated with Sylgard (Corning Inc.) and fire polished. Data were sampled at 20 or 100 kHz (depending on pulse durations) and filtered at 5 or 10 kHz, respectively, with an eight-pole low-pass Bessel filter. Data analysis was performed using self-written software (Visual C++; Microsoft Corp.) and the SigmaPlot program (Jandel Scientific).

Standard bath (internal) solution contained (mM): 120 NMDG-Cl, 2 $MgCl_2$, 10 HEPES, and 2 EGTA, pH 7.3, while standard extracellular (pipette) solution contained (mM): 100 NMDG-Cl, 5 $MgCl_2$, 10 HEPES, and 2 EGTA, pH 7.3. In the low external chloride solution, 90 mM of NMDG-Cl was replaced with 90 mM of NMDG-glutamate. pH was adjusted with NMDG or HCl to the desired value. Mutant I290M is described in Pusch et al. (1995b). RNA synthesis and oocyte injection were performed as described (Wollnik et al., 1997; Saviane et al., 1999).

Envelope Protocols

To separate the two gating processes at positive and negative voltages, we employed two different kinds of envelope protocols.

To evaluate the time constants of the gating processes at positive voltages, a long hyperpolarizing deactivating pulse to −140 mV was followed by short pulses of increasing duration to different potentials. The patch was then repolarized to −140 mV. Due to the capacity transient, the time course of current activation cannot be directly followed during the positive voltage step. Instead, we monitored the degree of activation as the initial current recorded upon repolarizing the patch to −140 mV, I_0. Clearly:

$$I_0 = N i_{-140} P_{open}(V_p;t_p), \quad (1)$$

where V_p is the prepulse potential, t_p is the time spent at V_p, N is the number of channels present in the patch and i_{-140} is the single channel amplitude at −140 mV.

I_0 was evaluated with the following procedure: the time course at −140 mV was fitted with a single exponential after the capacity transient; the fit was then extrapolated to the initial time of the pulse at –140 mV. Plotting I_0 as a function of t_p, we can measure the time dependence of the open probability of CLC-1 at V_p.

Since, at the highest voltages used, the fast gating process of CLC-1 has a time constant on the order of 10–20 μs, the speed of the voltage clamp might necessitate special consideration. In Fig. 1 A, we show the capacity artifact recorded when stepping from a holding potential of −140 to +200 mV when only the pipette holder, without pipette, was connected to the headstage of the EPC-7 amplifier (dashed line) or recorded from an inside-out patch from a noninjected oocyte, where the capacitive transient is due to membrane, pipette, and holder (solid line). As can be seen, the two have very similar time courses and comparable amplitudes. The large capacitive artifact of the holder (that has almost no influence on the actual charging time of the patch membrane, as it represents a capacity that is in parallel to the patch membrane) masks the actual charging of the membrane. It is thus evident that these current responses cannot be used to evaluate the speed with which the membrane is clamped. In the absence of a direct measure of the membrane voltage, the true "clamp-rise-time" can only be estimated based on the specifications of the manufacturer of the amplifier and the access resistance of the patch pipette and the capacity of patch membrane (see below).

To illustrate the procedure used in the analysis of the envelope protocol measurement and to demonstrate its robustness and independence of capacity artifacts, we show in Fig. 1 B an example of the extreme case of steps to V_p = +200 mV. Shown is a typical trace recorded with t_p = 180 μs. Three different fits were performed on this trace to show that the exact position of the cursors that limit the regime of fitting has very little influence on the time constants, as long as the initial capacity transient is avoided. The first analysis was done by fitting the curve between points indicated by arrows B and E with a single exponential and extrapolating the initial value to the point A (case 1). The use of a single instead of a double exponential function to fit the current trace in Fig. 1 B is justified by the relatively short duration of the repolarizing pulse compared with the slow time constant. Actually, even if we used a linear fit, we obtained practically identical results (not shown). For the second analysis, the curve was fitted between points D and E and extrapolated to C (case 2). Point C is clearly not the beginning of the repolarizing pulse, but even erroneously extrapolating the trace only to C instead of A has only a small effect on the evaluation of the time constant of activation (see below). The third fit was done between D and E and extrapolated to A (case 3). In Fig. 1 C, we show the initial currents recorded upon repolarization for the whole envelope protocol determined by using the cursor positions described above as a function of t_p. The initial values obtained in all three cases are very close, as are the time constants of the double exponential fits of the currents recorded upon repolarization: the fast time constant, τ_f, is 16, 17, and 17 μs, respectively. The slow time constant, τ_s, is 467, 456, and 462 μs, respectively.

A time constant of 16 μs, as estimated for the experiment described above, might be close to the limit of the clamp-rise-time. The patch-clamp amplifier itself has a finite rise time, which is on the order of 3.5 μs. Furthermore, if we assume, in the worst case,

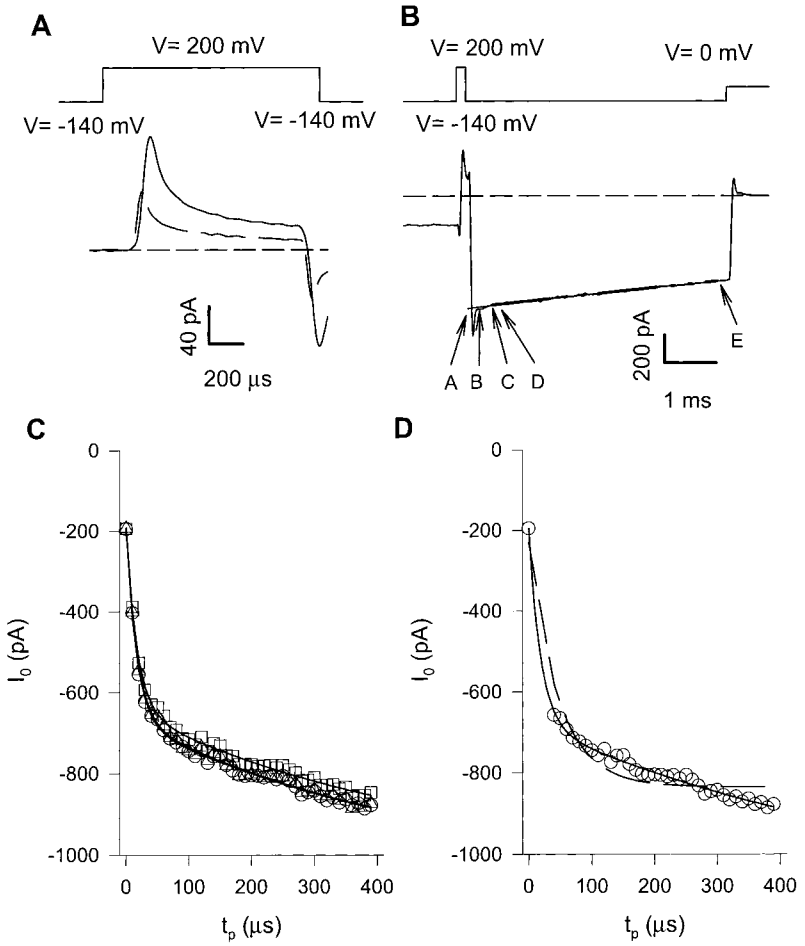

Figure 1. Limitations of the envelope protocols at high voltages. (A) Capacity artifact recorded when stepping from a holding potential of −140 to +200 mV for 1 ms due to a patch of a noninjected oocyte, the patch pipette and the holder (solid line), or from the pipette holder only (dashed line). (B) Typical current recorded with an envelope protocol to +200 mV, with t_p = 180 µs. Cursor positions used for the fitting are indicated by arrows: A = 0 (beginning of the repolarization pulse), B = 225 µs, C = 470 µs, D = 610 µs, and E = 4,775 µs. Three single-exponential fits were performed (that were superimposable). In the first (continuous line), the trace was fitted between B and E and extrapolated to A (set 1); in the second (thick dashed line, indistinguishable from the thick continuous line), the fit was done between D and E and extrapolated to C (set 2); in the third (not shown), the trace was fitted between D and E and extrapolated to A (set 3). (C) Initial currents recorded upon repolarization for a whole envelope protocol using set 1 of the cursor positions (○), set 2 (□) or set 3 (△). The continuous lines are double-exponential fits of the initial currents recorded upon repolarization in all three cases. Only two curves are clearly distinguishable since the traces corresponding to sets 1 and 3 are almost superimposable (and make up the thicker line), while the thinner visible curve corresponds to set 2. The time constants found are: τ_f(set 1) = 16 µs, τ_s(set 1) = 467 µs; τ_f(set 2) = 17 µs, τ_s(set 2) = 456 µs; τ_f(set 3) = 17 µs, τ_s(set 3) = 462 µs. (D) Double (continuous line) and the single (dashed line) exponential fit of the initial currents evaluated with set 1 of cursor positions but without the first three points (those with t_p = 10, 20, and 30 µs) to avoid contamination from phenomena of partial charging of the membrane. Clearly, a single-exponential function (dashed line) is inadequate to fit the data. The time constants obtained are τ_f = 19 µs and τ_s = 590 µs.

a patch capacitance of 2 pF and an access resistance of 5 MΩ, we would have a charging time constant estimated by $\tau_{clamp} = R_{pip}C_m$ = 10 µs. Therefore, the first few points in Fig. 1 C may be underestimates because the membrane is not yet fully charged after short pulse durations. To control for the possible degree of error introduced by this limitation, we performed a double exponential fit of the data points of Fig. 1 C (case 1) leaving out the first three points (those with t_p = 10, 20, and 30 µs) (Fig. 1 D). The time constants obtained in this way are τ_f = 19 µs and τ_s = 590 µs (Fig. 1 D, continuous line), showing that the first points are not essential to demonstrate the presence of two gating processes with very different kinetics. The large (37%) difference between the slow time constants is of no concern since, to obtain its correct value, longer pulses than those used in this example are needed anyway (see results). The fast time constants differ by ∼20%. From these considerations, it emerges that time constants faster than ∼20–30 µs are probably not precise measures and should be considered an upper limit of the true value because short pulses are not sufficient to fully charge the membrane to the desired value. However, this limitation concerns only a few data points at the upper extreme of the voltage range (see indication by the dashed line in Fig. 4).

At negative voltages, two distinct procedures to extract the gating time constant were used. Either the time course of the current was directly fitted with the sum of two exponentials, or the following protocol was used. After holding the patch at a positive potential (e.g., +60 mV) to fully activate the channels, the patch was clamped at a given potential, V_p, for increasing amounts of time, t_p. A brief step to +200 mV was given to fully saturate the fast gating process, and then the patch was repolarized to −140 mV. Under the hypothesis that the two gating processes are independent, the open probability of the channel is simply given by the product of the open probabilities of the two gating processes. Thus, the current recorded upon repolarization to −140 mV directly reflects the slow gate activation at V_p after t_p. In this way, it is possible to evaluate in isolation the time constant of the slow gating process. The time constant of the fast process can be deduced by fitting the time course of the currents at negative voltages with the product of two exponentials, with one time constant fixed to the value found previously for the slow process. The values obtained by the two different procedures agreed very well.

Deduction of Fast and Slow Gating Process Open Probability

If we assume that CLC-1 can conduct only if both gating processes are in the open state and that the two gating processes are independent, we can factorize the open channel probability into the product of the open probabilities of the two gating processes. With this assumption, we can measure at all voltages the open probabilities for the two gating processes using the following protocol: a long, 200-ms pulse at a given voltage (V_p) drives the channels in steady state. It is followed by a 10-ms repolarization to a

fixed potential of −140 mV. The initial current recorded upon repolarization will be

$$I(V_p) = Ni_{-140}P_o^s(V_p)P_o^f(V_p), \quad (2)$$

where $P_o^s(V_p)$ and $P_o^f(V_p)$ are the slow and fast gating process steady state open probability at V_p.

A short, 200-μs prepulse to +200 mV before the repolarizing pulse will maximally activate the fast gate while not substantially affecting the slow gate. This means that it can be safely assumed that $P_o^f = P_o^f(\max)$ while $P_o^s = P_o^s(V_p)$. Noise analysis measurements (Saviane et al., 1999) show that, at high positive voltages, $P_o^f(\max) \sim 1$. Assuming the latter condition, the initial current recorded upon repolarization will be $I_{pp}(V_p) = Ni_{-140}P_o^s(V_p)$, directly reflecting $P_o^s(V_p)$. The ratio of the initial currents in these two cases will thus give the fast gate open probability, $P_o^f(V_p)$: $I(V_p)/I_{pp}(V_p) = P_o^f(V_p)$.

We fitted the open probabilities obtained in this way using a Boltzmann function with an offset

$$f(V) = P_0 + \frac{1 - P_0}{1 + \exp\left[\frac{zF(V_{1/2} - V)}{RT}\right]}, \quad (3)$$

where P_o is the residual open probability at most negative voltages, $V_{1/2}$ is the half activation potential, and z is the apparent gating charge.

RESULTS

Separation of Fast and Slow Gating Processes in CLC-1

Fahlke et al. (1996) and Rychkov et al. (1996) have found that deactivation of CLC-1 at negative voltages could be fitted with the sum of two exponentials and a time-independent component. Fahlke et al. (1996) reported that the time constants of the two exponentials have similar values and do not have any appreciable voltage dependence. In contrast, Rychkov et al. (1996) described a slight voltage dependence of the two time constants. Our aim was to investigate the voltage dependence of the kinetics of CLC-1 over a wide voltage range, between −160 and +200 mV.

Fig. 2 A shows an example of typical currents recorded with an envelope protocol with V_p = 100 mV (see material and methods). The flat trace corresponds to the case where t_p = 0 ms. As can be seen, even a brief, 20 μs step to 100 mV is sufficient to induce a relatively large change in the initial current. Increasing the duration of the depolarizing pulse increases the initial current recorded at −140 mV. In Fig. 2 B are shown the initial current values as a function of t_p together with a double exponential fit (a single exponential fit is not adequate). The fast time constant in this case (100 mV) was 80 μs. To correctly evaluate the slower time constant, we used protocols similar to those described in Fig. 2, increasing prepulse duration in 100-μs steps instead of 10 μs. An example for V_p = 200 mV is shown in Fig. 3. The first trace in Fig. 3 A corresponds to t_p = 40 μs, a pulse duration that is sufficient to saturate the fast gating process at this voltage. In Fig. 3 B, the initial values of the currents recorded upon repolarization (●) are shown as a function of t_p. They can be well fitted with a single exponential (continuous line) with a time constant, τ_s, of 1.1 ms.

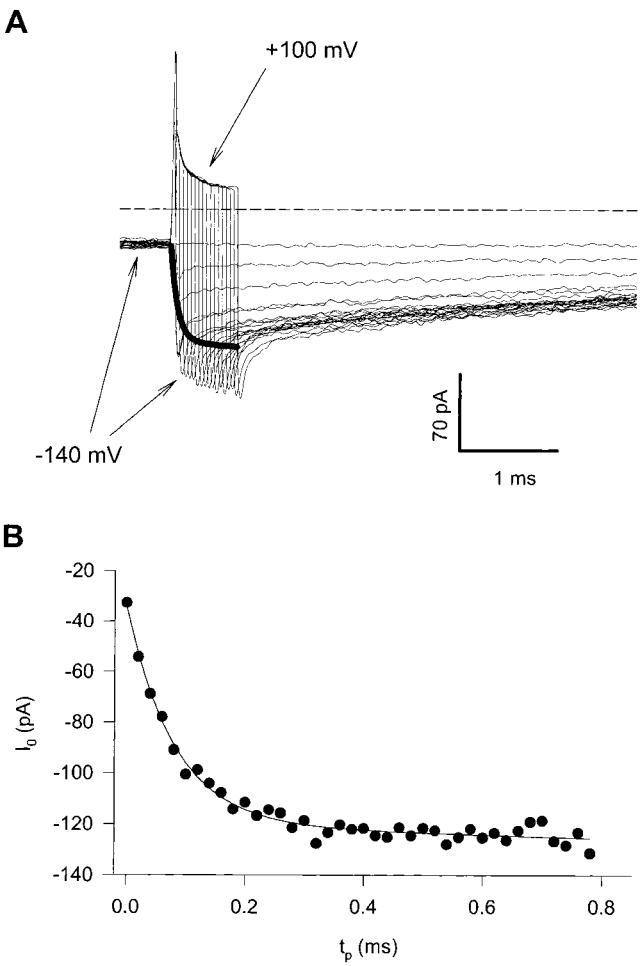

Figure 2. Separation of fast and slow gating process of CLC-1. (A) A 120-ms pulse to −140 mV is followed by a short pulse of varying duration to +100 mV, increasing its duration in 10-μs steps. The patch is then hyperpolarized to −140 mV for 15 ms. The thick line is a double-exponential fit of the initial currents recorded upon hyperpolarization to −140 mV. The initial part of the 120-ms pulse to −140 mV is not shown. Only every second trace is shown on the graph. Dashed line represents zero current. (B) Instantaneous currents recorded upon repolarization at −140 mV plotted as a function of the prepulse duration. The continuous line is a two-exponential fit with time constants of 80 μs and 3.4 ms.

In Fig. 4, the voltage dependence of the two time constants is shown (circles). At very positive voltages, they are about two orders of magnitude different (mean values at +200 mV: τ_f = 16 μs, τ_s = 1.0 ms). This difference decreases upon decreasing the applied potential until both time constants reach a plateau value (for V < −50 mV) and assume similar values τ_f(−140 mV) = 10 ms, while τ_s(−140 mV) = 27 ms, in agreement with previously published results (Fahlke et al.,

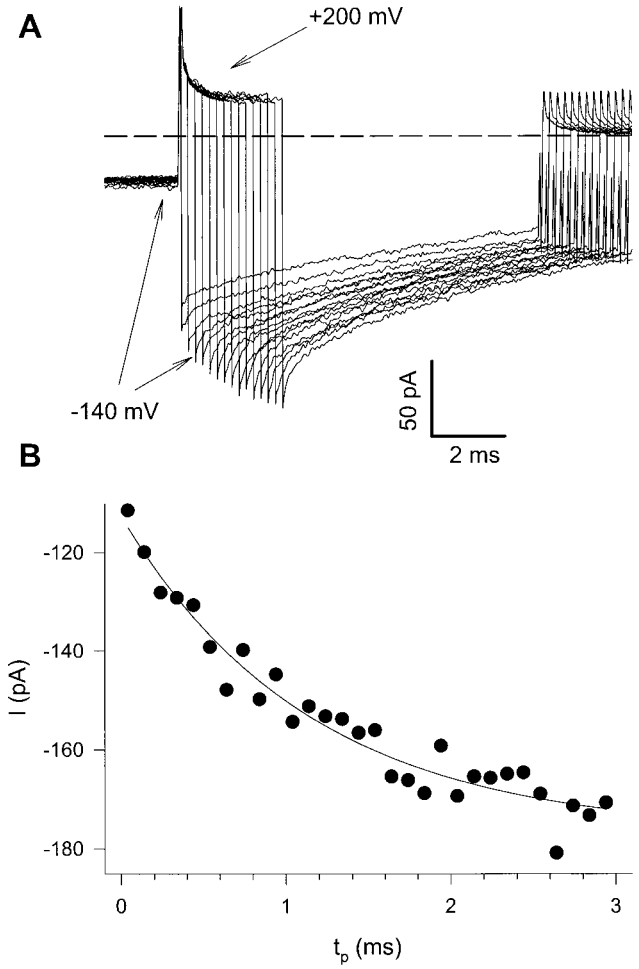

Figure 3. Determination of the slow time constant of CLC-1. (A) A 120-ms pulse to −140 mV is followed by a pulse of varying duration to +200 mV, increasing its duration in 100-μs steps starting from a minimum of 40 μs. The patch is then repolarized to −140 mV for 10 ms. The initial part of the 120-ms pulse to −140 mV is not shown. Only every second trace is shown on the graph. Dashed line represents zero current. (B) Instantaneous currents recorded upon repolarization at −140 mV plotted as a function of the prepulse duration. The fast gate is maximally activated by the prepulse, thus the recorded currents reflect only the slow gate activation. A single exponential fit gives a time constant of 1.1 ms.

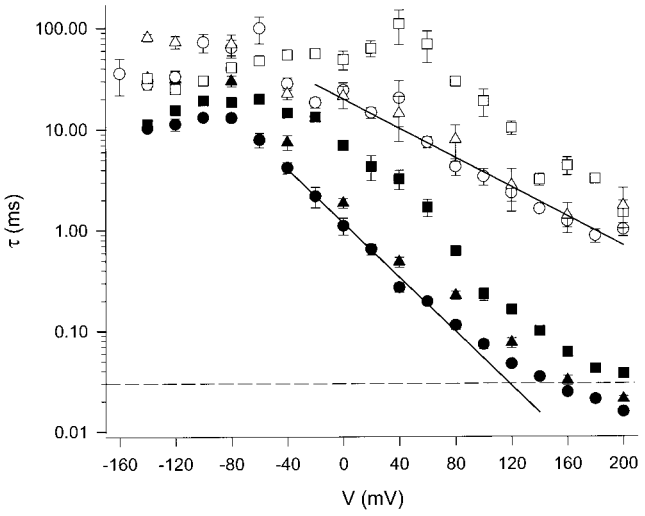

Figure 4. Fast and slow time constants as evaluated with envelope protocols are plotted as a function of voltage for different experimental conditions. Circles, standard conditions; squares, low external chloride; triangles, low internal pH (see materials and methods); filled symbols, fast gate time constants; open symbols, slow gate time constants. Error bars indicate SEM. Continuous lines are exponential fits (Eq. 4) of the fast and slow gate time constants in standard conditions yielding activation gating charges $z^{f}_{standard} = -0.79$ and $z^{s}_{standard} = -0.42$. Similar analysis was performed for low chloride and low pH also, but the fits are not shown. The dashed horizontal line indicates the limit of 30 μs. Data points below this value were not included in the fitting procedures because of possible limitations caused by a limited voltage clamp rise time (see materials and methods for details).

1996; Rychkov et al., 1996). For voltages more positive than −50 mV, the time constants associated to the fast gating process can be well fitted with a single exponential function (continuous line in Fig. 4):

$$\tau^{f}(V) = \tau^{f}(0)\exp(z^{f}FV/RT), \qquad (4)$$

where $\tau^{f}(V)$ is the fast gating process time constant at voltage V, F is Faraday's constant, R is the gas constant, T is the absolute temperature and z^{f} is the apparent "activation" gating charge of the fast gating process.

The limited clamp-rise-time that could cause the slight saturation at very high voltages, other than an intrinsic saturation of the channel, has been discussed in materials and methods. For these reasons, we have excluded time constants faster than 30 μs from the fit (Fig. 4, dashed line); i.e., the last three points ($V \geq +160$ mV) were not used. Under these approximations, we found that $z^{f}_{standard} = -0.79$.

For voltages larger than 0 mV, the voltage dependence of τ_s can also be well approximated with a single exponential function, the value obtained for the slow gating process apparent gating charge, $z^{s}_{standard}$, is −0.42.

Time Constant of the Fast Gate of CLC-0

The *Torpedo* chloride channel CLC-0 has two gates (Miller, 1982), a fast gate that has been shown to regulate single pore openings and a slow gate that regulates both pores simultaneously. The time constants of these processes are of the order of 10 ms for the fast gate at negative voltages and of seconds to minutes for the slow gate. To compare the fast gating process of CLC-1 with the fast gate of CLC-0, we used the same envelope protocols to evaluate its time constant. In Fig. 5 A are shown currents recorded when the patch is depolarized to +80 mV in pulses whose duration increases in 80-μs steps. The membrane is then repolarized back to −120 mV. The thick continuous line in Fig. 5 A is a single ex-

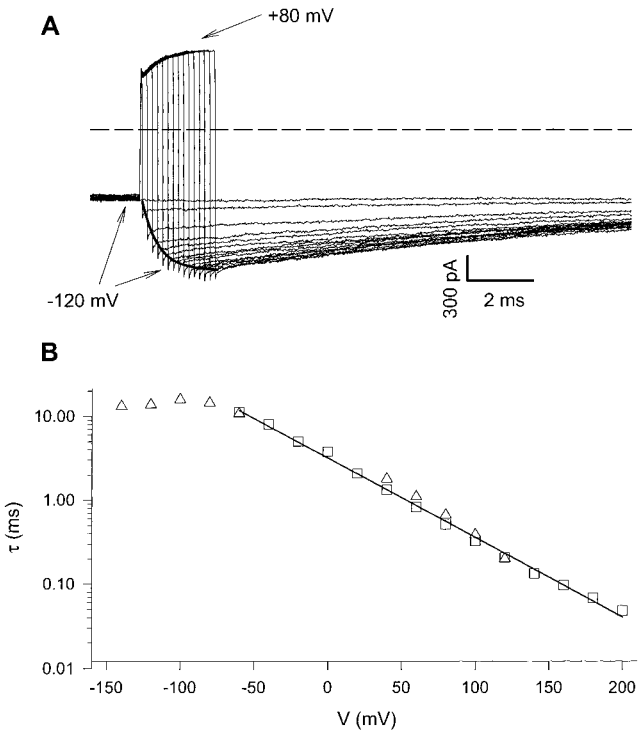

Figure 5. Evaluation of the fast gate time constant of CLC-0 with envelope protocols. (A) A 120-ms pulse to −120 mV followed by a pulse of varying duration to +80 mV is applied to the patch, increasing its duration in 80-μs steps. The patch is then hyperpolarized to −120 mV for 18 ms. The thick line is the single exponential fit of the initial values recorded upon repolarization. Its intercept with the current-trace reflects the best estimate of the initial current recorded upon repolarization. The downward "peak" of the individual traces is caused by the capacitive transient and thus does not faithfully reflect the ionic current flowing through the open channels (see also Fig. 1 B). The initial part of the 120-ms pulse to −120 mV is not shown. The dashed line represents zero current. (B) Time constants of the fast gate of CLC-0 measured both with envelope protocols (□) and by direct fitting of the current during the activation pulse (△). The continuous line is a single exponential fit (Eq. 4) of the fast gate time constants that yields $z^{f}_{CLC\text{-}0} = -0.55$.

ponential fit of the initial currents recorded upon repolarization. The degree of activation of the fast gate of CLC-0 was measured by both monitoring the initial current recorded upon repolarization (Eq. 1) and, for V ≤ +120 mV, directly fitting the time course of the current with a single exponential function. These two methods give independent measurements of the time constant of the fast gate of CLC-0, and the results at all investigated voltages are shown in Fig. 5 B. The agreement between the values for the fast gate time constant found by directly fitting the time course (△) or with the envelope protocols (□) is very good. More interesting is to observe that τ_f(CLC-0) and τ_f(CLC-1) have the same qualitative behavior: at negative voltages they have almost constant values, while upon rising the applied potential they become increasingly faster without showing saturation even at the highest tested voltages (+200 mV), although τ_f(CLC-0) is ∼10 times slower than τ_f(CLC-1). For voltages more positive than −60 mV, the voltage dependence of τ_f(CLC-0) can be well approximated with a single exponential function giving a gating charge value, $z^{f}_{CLC\text{-}0}$, of −0.55, a value that is slightly smaller than that obtained for the fast gating process of CLC-1, $z^{f}_{CLC\text{-}1} = -0.79$.

Fast and Slow Gate Open Probabilities

We used the pulse protocols described in materials and methods to separate the voltage dependence of the fast and slow gates. Fig. 6 A shows typical tail currents recorded when, after 200-ms pulses to various V_p, the voltage is immediately stepped to −140 mV. In Fig. 6 B are shown the currents recorded from the same patch when the voltage is stepped to +200 mV for 200 μs to fully activate the fast gate before the −140-mV repolarization. With these protocols, we are able to separate the steady state open probabilities of the fast and slow gating processes at V_p (see materials and methods). We fitted the open probabilities obtained in this way (Fig. 6 C) to a Boltzmann function with an offset (Eq. 3).

At very negative potentials, both gating processes have nonzero open probabilities, 0.16 and 0.65 for the fast (Fig. 6 C, ▲) and slow (○) gates, respectively. The behavior of the fast process is very similar to that of the fast gate of CLC-0; at very negative potentials, the open probability of the fast gate does not become zero, but reaches a minimum value of 0.25 (Chen and Miller, 1996; Ludewig et al., 1997a).

To separate the open probabilities of the two gating processes, we assumed their mutual independence. A simple consideration shows that even without this strong hypothesis most of our analysis remains correct.

Our measurements show that at high positive voltages the time constants characterizing the two gating processes are very different. Thus, during a short activating pulse to high voltages, the slow gate can be considered fixed, while the fast gate of those channels with an open slow gate reaches equilibrium. A simple double-barreled channel with a slow gate that regulates both protopores simultaneously and two fast gates, which we will assume to be independent once the slow gate is open, that regulate single protopore openings has six possible states, S_0–S_5, of which only two are conductive (S_4 and S_5; see Fig. 7). The current recorded upon repolarization with the regular tail protocols, $I(V_p)$, will be proportional to $p_{S_4}(V_p) + 2p_{S_5}(V_p)$, where $p_{S_4}(p_{S_5})$ is the probability that the channel is in state S_4 (S_5) at voltage V_p. A brief prepulse to +200 mV will open the fast gates of those channels that have an open slow gate, while the state of the slow gate remains unchanged. Thus, the current recorded upon repolarization with prior prepulse, I_{pp}, will reflect all channels with an open slow gate:

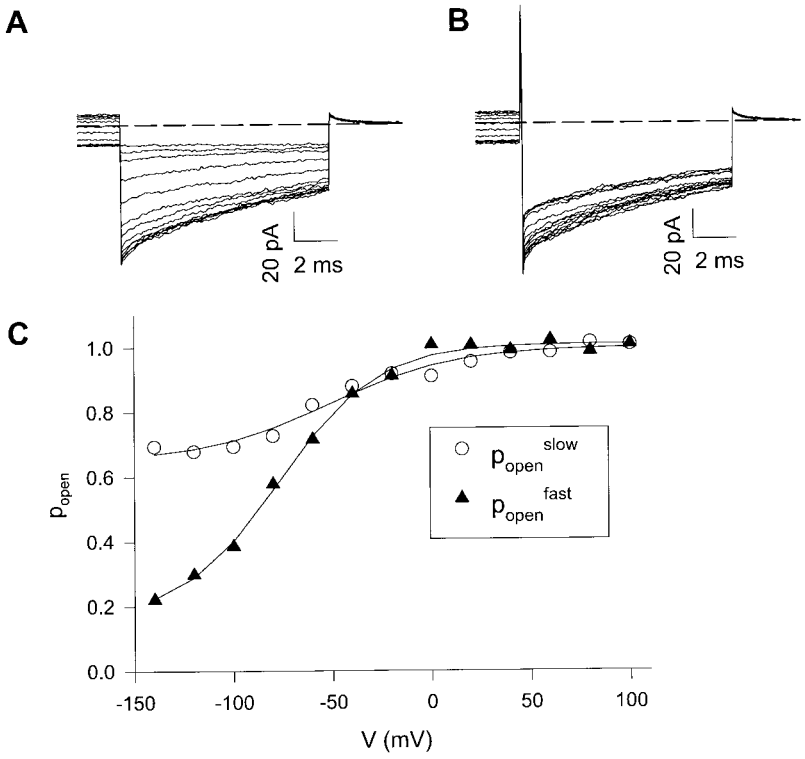

Figure 6. Separation of fast and slow gate open probabilities. (A) Currents recorded when 200-ms pulses of increasing voltages from −140 to +100 mV are followed by a 10-ms repolarization to −140 mV. The initial part of the 200-ms pulse to −140 mV is not shown. Dashed line represents zero current. (B) Currents recorded when 200-ms pulses of increasing voltages from −140 to +100 mV are followed by a short 200-μs pulse to +200 mV, and then by a 10-ms repolarization to −140 mV. The initial part of the 120-ms pulse to −140 mV is not shown. Dashed line represents zero current. (C) Open probabilities for the fast (▲) and slow (○) gating processes. Continuous lines are the fits of the open probabilities with Eq. 3. The obtained values are: $P_0^f = 0.16$, $V_{1/2}^f = -77$ mV; and $z^f = 1.03$, $P_0^s = 0.65$, $V_{1/2}^s = -51$ mV, and $z^s = 0.81$.

$I_{pp}(V_p) \propto 2(p_{S_3} + p_{S_4} + p_{S_5}) = 2p_S(V_p)$. If the fast gate is significantly more rapid than the slow gate, the three open-slow-gate states, $S_{3\text{-}5}$ in Fig. 7, will equilibrate among each other quickly after each opening of the slow gate, and their respective occupation probability will follow a (conditioned) binomial distribution, since we have assumed that the fast gates are independent:

$$\begin{aligned} p_{S_3} &= p_S(1-p_{f+})^2 \\ p_{S_4} &= 2p_S p_{f+}(1-p_{f+}) \\ p_{S_5} &= p_S p_{f+}^2, \end{aligned} \tag{5}$$

where p_S is the total open probability of the slow gate, and p_{f+} is the conditional probability that a fast gate is open given that the slow gate is open. Using these relations (Eq. 5), it follows that $I_{pp}(V_p) \propto p_S(V_p)$ and $I(V_p) \propto p_S(V_p)p_{f+}(V_p)$. Thus the current recorded upon repolarization in the tail current protocols with the prepulse to +200 mV, I_{pp}, will be directly proportional to the slow gating process open probability at V_p, exactly as it was under the independent gating assumption, and the ratio:

$$\frac{I(V_p)}{I_{pp}(V_p)} = p_{f+}(V_p)$$

is the conditional open probability of the fast gate given that the slow gate is open. As discussed above, the latter relation is strictly valid only with the condition that the fast gate is "significantly" more rapid than the slow one. This is certainly a good assumption for voltages more positive than −40 mV, for which the fast gate is at least ~10-fold faster. Below this value, the assumption is, however, still approximately valid, because the kinetic difference reaches a ratio of $\tau_s/\tau_f \sim 3$ at negative voltages.

These results are remarkably similar to those obtained under the independent gate hypothesis (Eq. 2). Thus, this hypothesis is not crucial; rather, the really fundamental assumption for the interpretation of our data (apart from the double-barrel assumption) is the independence of the two fast protopore gates once the slow gate is open.

Effect of Chloride Concentration, Internal pH, and Mutation I290M on the Two Gating Processes of CLC-1

Lowering the internal pH and the external chloride has opposite effects on the open probability of CLC-1 (Rychkov et al., 1996; Saviane et al., 1999), and the dominant myotonia-inducing mutation, I290M, induces a strong shift of the apparent open probability towards depolarizing potentials (Pusch et al., 1995b; Saviane et al., 1999). However, these effects have been studied only in a limited voltage range and the effects on the different gating processes have not been investigated in detail. We sought to investigate the differential effects of changing these experimental conditions on the two gating processes. We lowered the external chloride concentration from 110 to 20 mM and the internal pH from 7.3 to 6.5. To evaluate the time constants of

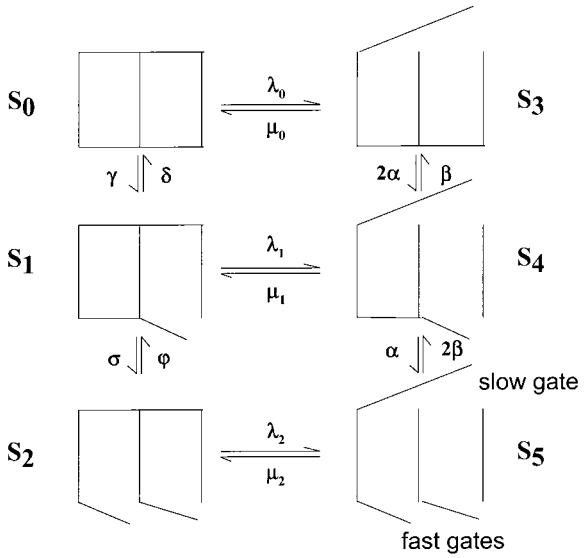

Figure 7. Double-barreled model for CLC-1. Channel opening is governed by two types of gates, one common pore gate (slow gate) and two protopore gates (fast gates). States S_0–S_2 are nonconducting, because the slow gate is closed. State S_3 is nonconducting because both fast gates are closed. The conductance of state S_5 is twice that of S_4. The fast gates are independent of each other with the slow gate open, whereas all other transition rates depend on the channel state.

the two gating processes in 20-mM external chloride and at pH_{int} 6.5, we used the same protocols described above. Time constants found for low $[Cl^-]_{ext}$ and low pH_{int} are shown in Fig. 4. Lowering the external chloride concentration (Fig. 4, squares) has the effect of slowing both gating processes, while lowering the internal pH from 7.3 to 6.5 (triangles) has only a minor effect on the time constants characterizing the two gating processes. The apparent activation gating charge associated with the fast gating process (Eq. 4) does not vary much, either changing the external chloride concentration to 20 mM or lowering the internal pH to 6.5; in fact, the values obtained in these cases are $z_{low\ Cl}{}^f = -0.68$ and $z_{low\ pH}{}^f = -0.79$, respectively, as compared with $z_{standard}{}^f = -0.79$. For the slow gating process, lowering the internal pH and the external chloride concentration had only small effects on the apparent activation gating charge ($z_{low\ pH}{}^s = -0.31$; $z_{low\ Cl}{}^s = -0.68$).

To measure the steady state open-probabilities, protocols similar to those described in Fig. 6, A and B, were applied with typical current traces shown in Fig. 8 in different experimental conditions. The duration of the prepulse at +200 mV varied depending on the experimental condition as the time needed to fully saturate the fast gating process depends upon the experimental condition (40 μs in the low internal pH condition, 1 ms for the I290M mutation, and 100 μs for low external chloride). The fast and slow gating process open probabilities found were then fitted with a Boltzmann curve with an offset (Eq. 3). The results are summarized in Fig. 9.

Lowering the external chloride concentration from 110 to 20 mM leads to a rightward shift in the half activation potential of both gates. The slow gate's half activation potential, $V_{1/2}{}^s$, shifts by almost 47 mV, while the fast gate $V_{1/2}{}^f$ shifts by 27 mV. The residual open probability of the fast gate, $P_0{}^f$, at very negative voltages is unaffected, while the slow gate's $P_0{}^s$ is reduced by almost 40%.

The effects due to the lowering the internal pH to 6.5 are less pronounced, and in the opposite direction than those induced by lowering external chloride. The half-activation potential of both gates is shifted towards hyperpolarizing potentials by ~20 mV, while the residual open probability at very negative voltages of both gates is increased, although to a lesser extent for the slow gate (+14%) than for the fast gate (+36%).

The dominant myotonia-inducing mutation, I290M, has a very strong effect on the half activation potential. It raises $V_{1/2}{}^s$ to 35.6 ± 5.5 mV, a shift of >100 mV towards more positive potentials, while raising $V_{1/2}{}^f$ by almost 74 mV. This mutation also lowers the residual open probabilities of the fast and slow gates by 14 and 34%, respectively.

DISCUSSION

This paper presents evidence that CLC-1 has two gating processes, which are voltage dependent over the whole voltage range from −160 to +200 mV. While at negative voltages the time constants are quite similar, for voltages higher than −50 mV they grow apart, and at +200 mV they are about two orders of magnitude different, τ_f = 16 μs and τ_s = 1 ms, respectively, mimicking very well the difference between the time constants of the two gates in CLC-0, τ_s(CLC-0) ~ 1–100 s, while τ_f(CLC-0) ~ 10 ms (Ludewig et al., 1997a; Pusch et al., 1997).

Fahlke et al. (1996) suggested that CLC-1 has two distinct gating processes that are voltage independent for voltages between −175 and −45 mV. Other groups (Rychkov et al., 1996) reported that the time constants did show some voltage dependence in that limited range of potentials, but still it was not possible to clearly separate the voltage dependence of the two gating processes. In this paper, we show that CLC-1 has two distinct voltage-dependent processes that are characterized by time constants of similar value for voltages lower than −50 mV, while at more positive potentials they have an exponential voltage dependence with apparent activation gating charges of $z^f_{standard} = -0.79$ and $z^s_{standard} = -0.42$. The exponential voltage dependence that we observe for voltages greater than −40 or 0 mV for the fast and slow gate, respectively, lie in a voltage range that had not been previously investigated by others (Fahlke et al., 1996; Rychkov et al., 1996). Limited to voltages more negative than −40 mV, our data agree with the

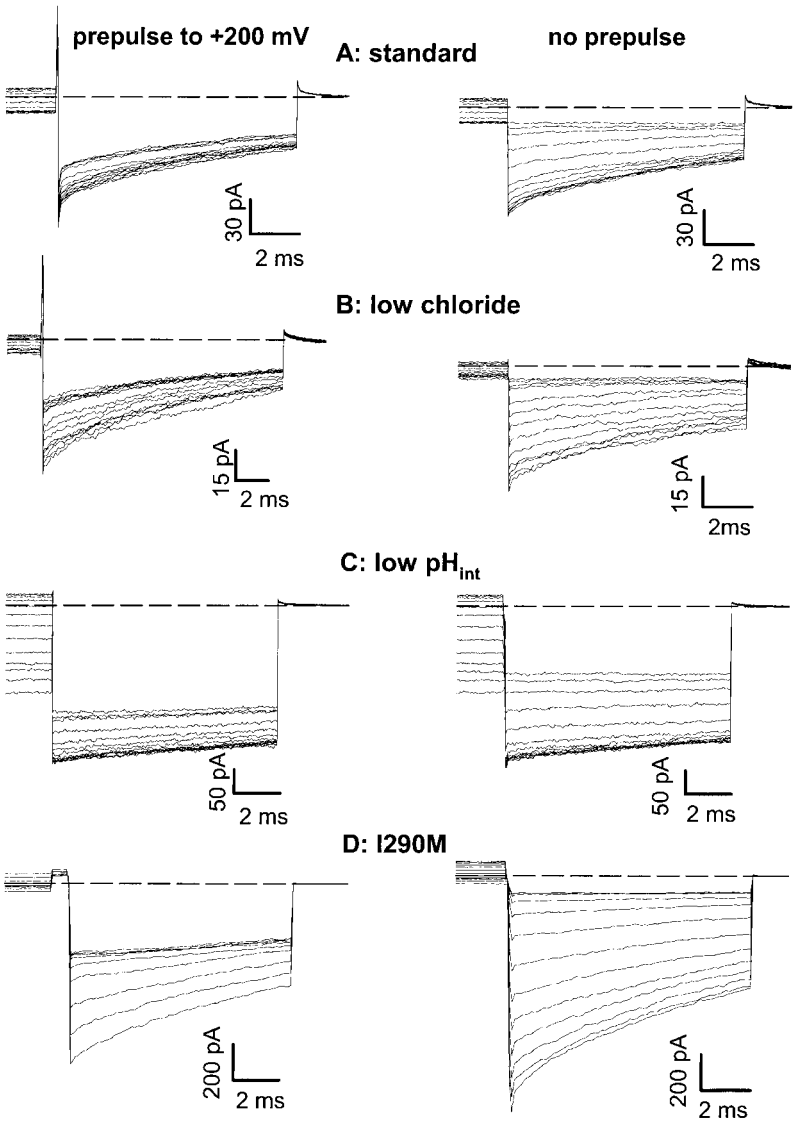

Figure 8. Currents evoked with protocols similar to those described in Fig. 6, A and B, in different experimental conditions. The stimulation protocol in the left column is a 200-ms pulse at voltages varying from −140 to +100 mV in 20-mV steps, followed by a short activating pulse at +200 mV whose duration is sufficient to fully activate the fast gate in the different conditions, and then followed by a 10-ms repolarization to −140 mV. The stimulation protocol in the right column is the same, except that there is no activating pulse at +200 mV. The initial part of the 200-ms pulse to the varying potential is not shown. Dashed line represents zero current. (A) Standard conditions. (B) Low external chloride solution, 20 mM. (C) Low internal pH 6.5. (D) Dominant myotonia inducing mutation, I290M.

previously published results (Fahlke et al., 1996; Rychkov et al., 1996) in that the two processes show little voltage dependence and have similar time constants.

Is an Ultrafast Gate Needed for CLC-1?

In a previous model of gating of CLC-1, Fahlke et al. (1996) proposed that CLC-1 has a completely different gating mechanism than CLC-0 based on two conventional voltage sensors that can move between two possible states and reach equilibrium on a very fast time scale ("ultrafast gate") that determine the voltage dependence. They justified the three current components (fast and slow deactivating and nondeactivating) with the possible combinations of the positions of the voltage sensors. The opening and closing of the channel in their model is voltage independent and regulated by a cytoplasmic gate similar to the "ball and chain" proposed by Armstrong and Bezanilla (1977) for the K^+ channel.

The presence of this "ultrafast" gating mechanism was inferred mainly from two observations. First, the instantaneous I-V relationship measured after conditioning pulses at −30 or −85 mV differed only at negative voltages, while at positive potentials they were almost indistinguishable (see Figure 4 A in Fahlke et al., 1996). Second, they observed no increase in the current during short positive pulses, even though the initial current after repolarization was increased (see Figure 4 B in Fahlke et al., 1996). Both observations can be easily accounted for without the ad-hoc assumption of an ultrafast gating process. The first observation can be explained by noticing that for positive voltages both time constants are very fast and thus it is not possible to directly monitor any kind of relaxation since the capacitative transient due to the cell itself masks the activation process. In a similar way, the second observation can be explained by the fact that the above mentioned capacitative transient masks the fast gate activation of CLC-1.

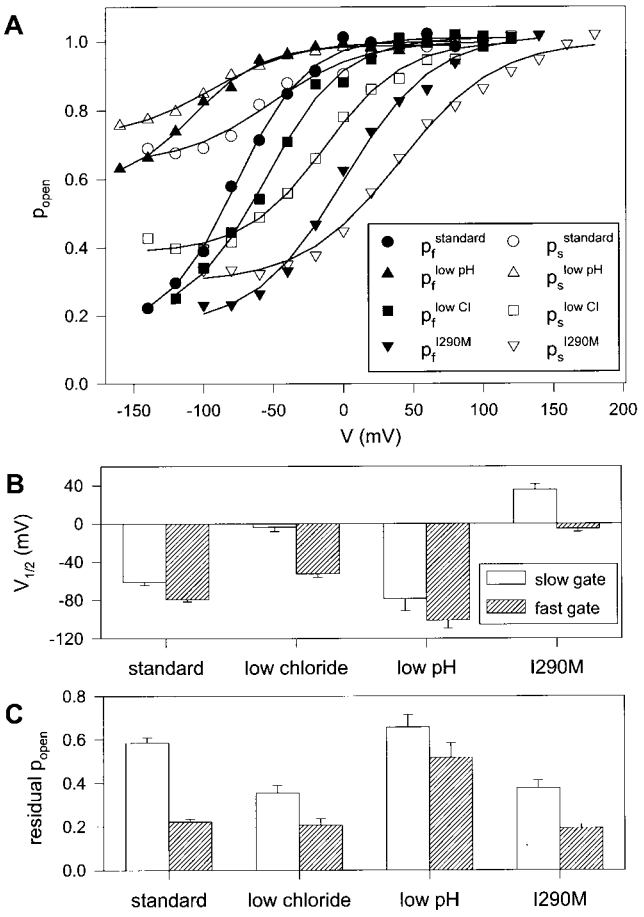

Figure 9. Fast and slow gate open probabilities in different experimental conditions. (A) Boltzmann fits (continuous lines) of the mean values of the fast (filled symbols) and (empty symbols) slow gating process open probabilities in different conditions. Circles, standard solution; squares, low extracellular chloride; triangles, low intracellular pH; inverted triangles, I290M mutation. (B) Half activation potentials for the fast and slow gate in the different experimental conditions described above. (C) Residual open probability at most negative voltages for the fast and slow gate in the different experimental conditions described above. Shaded histograms relative to fast gate parameters and empty histograms relative to slow gate parameters.

Moreover, our data clearly show that the two gating processes identified at negative voltages (Pusch et al., 1994; Fahlke et al., 1996; Rychkov et al., 1996) become increasingly faster when the applied voltage is increased. It is thus possible to identify the ultrafast gating process postulated by Fahlke et al. (1996) at positive voltages with the "normal" fast gating process, since at high positive voltages τ_f becomes so small that it could not be identified by direct measurements for the reasons discussed above. Moreover, Fahlke's model implies a non-Markovian kinetic scheme. This non-Markovian behavior was postulated based on their finding that the time constants are not voltage dependent. Here, we clearly demonstrate a strong voltage dependence of both time constants, definitely ruling out the model of Fahlke et al. (1996). Our results are more consistent with a simpler Markovian kinetic scheme of the type shown, for example, in Fig. 7.

Possible Mechanism of Cl^--dependent Gating of CLC-0 and CLC-1

It has been proposed that the Cl^- ion acts as the gating particle for the fast gate of CLC-0 (Pusch et al., 1995a; Chen and Miller, 1996) and also for CLC-1 (Rychkov et al., 1996). The mechanism by which Cl^- gates the channel is still largely unknown. Pusch et al. (1995a) speculated that the permeation pore can contain two distinct anion binding sites and the fast gate is close to the cytoplasmic side of the membrane. Occupation of the internal binding site shifts the equilibrium between open and closed conformations to the open state. This model assumes that the voltage-dependent step is the Cl^- movement from the outer site to the inner one. For the following reasons, this model implies that the fast gate time constant should saturate as a function of voltage. At positive voltages, the fast gate opening rate, α, would have the following form: $\alpha = p_{Cl}\alpha_{Cl}\ 1\ (1 - p_{Cl})\alpha_0$, where p_{Cl} is the probability of having a bound Cl^- ion inside the channel, α_{Cl} is the opening rate of the channel with a bound chloride ion, and α_0 is the opening rate without a bound chloride ion. Binding should saturate at positive voltages ($p_{Cl} \sim 1$) and thus $\alpha \sim \alpha_{Cl}$ (i.e., the activation time constant) should saturate as a function of voltage at the value $\tau_f = 1/\alpha_{Cl}$. Chen and Miller (1996) proposed another model for CLC-0 that assumes the presence of two closed states to which Cl^- ions can bind and that are separated by a conformational change such that the Cl^- ion is moved inwards into the voltage gradient, possibly through a geometrical rearrangement in the permeation pathway that is electrically equivalent to an inward movement of Cl^-. This model predicts that τ_f does not saturate at any voltage since the voltage-dependent step is not dependent on the ionic concentration. Here we have shown that, for CLC-0, there is no saturation of τ_f up to +200 mV (Fig. 5). This result strongly suggests that the opening step of a single CLC-0 protopore is directly associated with a transmembrane charge movement. Thus, a model like the one proposed by Chen and Miller (1996) is probably more suited to realistically describe the gating mechanism of CLC-0 by the Cl^- ion. The qualitative similarity of the voltage dependence of the fast time constant of CLC-1 indicates that a model similar to that of Chen and Miller (1996) could also describe the fast gating of CLC-1.

Identification of the Fast and Slow Gating Processes of CLC-1 with the Fast and Slow Gate of CLC-0

The single-channel analysis performed by Saviane et al. (1999) showed that CLC-1 has three equidistant con-

ductance states. Their analysis is consistent with the hypothesis that CLC-1 has two fast gates, regulating the transitions between the three conductance states, and a slower gate that additionally modulates the permeation pathway. These observations strongly suggest a double-barreled structure for CLC-1. The values of the open probabilities that Saviane et al. (1999) found from single-channel measurements (SC) for the fast and slow gates and those obtained for the fast and slow gating processes from our macroscopic currents measurements (MC) are remarkably similar: at V = −140 mV and pH_{int} 6.5, Saviane et al. (1999) reported that $P_o^{f,\,SC} = 0.59$ and $P_o^{s,\,SC} = 0.69$, while we find that $P_o^{f,\,MC} = 0.66$ and $P_o^{s,\,MC} = 0.76$; for the time constants, in the same conditions, single-channel analysis yields $\tau_f^{SC} = 17$ ms and $\tau_s^{SC} = 51$ ms, while we find $\tau_f^{MC} = 33$ ms and $\tau_s^{MC} = 81$ ms. This agreement suggests that the two macroscopically identified gating processes correspond to the two microscopically identified gates.

Pusch et al. (1995a) have shown that reducing the external chloride concentration from 100 to 22 mM induces a right shift of ~30 mV in the $V_{1/2}$ of the fast gate of CLC-0, a value close to what we find, in similar conditions, for the shift of $V_{1/2}$ of the fast process of CLC-1 (27 mV). For CLC-0, there is no quantitative analysis of the slow-gate dependence on $[Cl^-]_{ext}$, but Chen and Miller (1996) clearly showed that lowering $[Cl^-]_{ext}$ induces reduction of the open probability of the slow gate (see Figures 4 and 5 in Chen and Miller, 1996). This is also consistent with what we observe in our conditions for the slow process of CLC-1.

Our findings agree also with the results of Hanke and Miller (1983) on the pH dependence of the fast gate of CLC-0. Lowering the pH_{int} increases the open probability of the fast gate for both CLC-0 and CLC-1.

One of the most characterizing features of CLC-0 is that it never closes completely and at most negative voltages the fast gate open probability is non-zero, P_0(CLC-0) = 0.25 (Chen and Miller, 1996; Ludewig et al., 1997a). The fast gating process of CLC-1 shares this peculiarity with the fast gate of CLC-0; in fact, we find that its open probability is always non-zero and at most negative voltages is 0.16, a value similar to that of CLC-0.

All these phenomenological similarities suggest that the fast gating process of CLC-1 can be identified with the fast gate of CLC-0 and the slow process with the slow, common pore gate. A major difference of the slow process of CLC-1 compared with the slow gate of CLC-0 is the direction of the voltage dependence. However, several point mutations of CLC-0 also abolish or invert the voltage dependence of the slow gate of CLC-0 (Ludewig et al., 1996; our unpublished results). Further experiments using, for example, mutants that specifically affect one of the gates could help to verify this conclusion.

In summary, we find that gating of CLC-1 is governed by two voltage-dependent processes that differ in kinetics by almost two orders of magnitude at large positive voltages and that most likely correspond to the single protopore and the common pore gate of the double-barreled channel. The large kinetic difference allows a fairly good separation of these processes.

We thank T.J. Jentsch for kindly providing the cDNAs.

This study was partially supported by Telethon, Italy (grant 1079 to M. Pusch) and by the Italian CNR Progetto Strategico Biosensori.

Submitted: 27 March 2000
Revised: 26 July 2000
Accepted: 31 July 2000

REFERENCES

Armstrong, C.M., and F. Bezanilla. 1977. Inactivation of the sodium channel. II. Gating current experiments. *J. Gen. Physiol.* 70:567–590.

Chen, T.Y., and C. Miller. 1996. Nonequilibrium gating and voltage dependence of the CLC-0 Cl^- channel. *J. Gen. Physiol.* 108:237–250.

Fahlke, C., T. Knittle, C.A. Gurnett, K.P. Campbell, and A.L. George, Jr. 1997. Subunit stoichiometry of human muscle chloride channels. *J. Gen. Physiol.* 109:93–104.

Fahlke, C., T.H. Rhodes, R.R. Desai, and A.L. George, Jr. 1998. Pore stoichiometry of a voltage-gated chloride channel. *Nature.* 394: 687–690.

Fahlke, C., A. Rosenbohm, N. Mitrovic, A.L. George, and R. Rüdel. 1996. Mechanism of voltage-dependent gating in skeletal muscle chloride channels. *Biophys. J.* 71:695–706.

Hamill, O.P., A. Marty, E. Neher, B. Sakmann, and F.J. Sigworth. 1981. Improved patch clamp techniques for high-resolution current recording from cells and cell-free membrane patches. *Pflügers Arch.* 391:85–100.

Hanke, W., and C. Miller. 1983. Single chloride channel from *Torpedo* electroplax: activation by protons. *J. Gen. Physiol.* 82:25–45.

Jentsch, T.J., K. Steinmeyer, and G. Schwarz. 1990. Primary structure of *Torpedo marmorata* chloride channel isolated by expression cloning in *Xenopus* oocytes. *Nature.* 348:510–514.

Koch, M.C., K. Steinmeyer, C. Lorenz, K. Ricker, F. Wolf, M. Otto, B. Zoll, F. Lehmann-Horn, K.-H. Grzeschik, and T.J. Jentsch. 1992. The skeletal muscle chloride channel in dominant and recessive human myotonia. *Science.* 257:797–800.

Ludewig, U., T.J. Jentsch, and M. Pusch. 1997a. Analysis of a protein region involved in permeation and gating of the voltage-gated chloride channel ClC-0. *J. Physiol.* 498:691–702.

Ludewig, U., M. Pusch, and T.J. Jentsch. 1996. Two physically distinct pores in the dimeric CLC-0 channel. *Nature.* 383:340–343.

Maduke, M., D.J. Pheasant, and C. Miller. 1999. High-level expression, functional reconstitution, and quaternary structure of a prokaryotic ClC-type chloride channel. *J. Gen. Physiol.* 114:713–722.

Middleton, R.E., D.J. Pheasant, and C. Miller. 1996. Homodimeric structure of a ClC-type channel. *Nature.* 383:337–340.

Miller, C. 1982. Open-state substructure of single chloride channels from *Torpedo* electroplax. *Phil. Trans. R. Soc. Lond. B Biol. Sci.* 299: 401–411.

Pusch, M., U. Ludewig, and T.J. Jentsch. 1997. Temperature dependence of fast and slow gating relaxations of ClC-0 chloride channels. *J. Gen. Physiol.* 109:105–116.

Pusch, M., U. Ludewig, A. Rehfeldt, and T.J. Jentsch. 1995a. Gating of the voltage-dependent chloride channel ClC-0 by the permeant anion. *Nature.* 373:527–531.

Pusch, M., K. Steinmeyer, and T.J. Jentsch. 1994. Low single channel conductance of the major skeletal muscle chloride channel, ClC-1. *Biophys. J.* 66:149–152.

Pusch, M., K. Steinmeyer, M.C. Koch, and T.J. Jentsch. 1995b. Mutations in dominant human myotonia congenita drastically alter the voltage-dependence of the ClC-1 chloride channel. *Neuron*. 15:1455–1463.

Rychkov, G.Y., M. Pusch, D.St.J. Astill, M.L. Roberts, T.J. Jentsch, and A.H. Bretag. 1996. Concentration and pH dependence of skeletal muscle chloride channel ClC-1. *J. Physiol.* 497:423–435.

Saviane, C., F. Conti, and M. Pusch. 1999. The muscle chloride channel ClC-1 has a double-barreled appearance that is differentially affected in dominant and recessive myotonia. *J. Gen. Physiol.* 113:457–467.

Steinmeyer, K., C. Ortland, and T.J. Jentsch. 1991. Primary structure and functional expression of a developmentally regulated skeletal muscle chloride channel. *Nature.* 354:301–304.

Wollnik, B., C. Kubisch, K. Steinmeyer, and M. Pusch. 1997. Identification of functionally important regions of the muscular chloride channel ClC-1 by analysis of recessive and dominant myotonic mutations. *Hum. Mol. Genet.* 6:805–811.